Heliyon 6 (2020) e03275

Contents lists available at ScienceDirect

Heliyon

journal homepage: www.cell.com/heliyon

Research article

Comparative study of mechanical properties of cast and forged Al-3Mg-MnO_2 and Al-8Mg-MnO_2 composites

Vikas Narain [a,*], Subrata Ray [b]

[a] Shri Bhawani Niketan Institute of Technology and Management, India
[b] Indian Institute of Technology Mandi, India

ARTICLE INFO

Keywords:
Materials science
Metallurgical engineering
Al-Mg-MnO_2 composite
Initial fracture toughness
Growth toughness
Hardness
Elongation
Yield strength
Tensile strength

ABSTRACT

The Al-Mg-MnO_2 composite is a MnO_2 particulate reinforced Al metal matrix composite. Its substantial ductility makes it promising composite for study. The Al-3Mg-MnO_2 and Al-8Mg-MnO_2 composites were synthesized by stirring 3, 5, and 8 wt% of MnO_2 particulates in Al-3Mg melt and Al-8Mg melt to study their mechanical properties. Their microstructure shows intermetallic precipitates of Al, Mg, and Mn at dendrites, grain boundaries and within the grains. In both sets of composites, the hardness, and the yield strength increases with increasing MnO_2 content in the cast and forged composites. Both the groups of composites show an increase in tensile strength with increasing particle content from 3 to 5 wt%, a further increase in particle content to 8 wt%, leads to an abrupt decrease in tensile strength in both the group of composites. The percentage elongations in forged composites are lower than those in cast composites, but this decrease is more prominent in Al-8Mg-MnO_2 composites in comparison to Al-3Mg-MnO_2 composites. The J_{IC} value decreases as the percentage of MnO_2 particles increases in Al-3Mg-MnO_2 and Al-8Mg-MnO_2 composites. Forging increases J_{IC} values in both the class of composites in comparison to their cast counterparts due to work hardening and healing of pores. Crack growth toughness also decreases as the MnO_2 particle content increases in Al-3Mg-MnO_2 and Al-8Mg-MnO_2 composites. Forged Al-3Mg-MnO_2 shows decreased T/E ratio in comparison to their cast counterparts except at 8wt%. However, forged Al-8Mg-MnO_2 shows improved T/E at 3wt% and a drop at 5wt% and 8wt% MnO_2. Variation of crack growth toughness between cast and forged Al-8Mg-MnO_2 is minimal in comparison to that between cast and forged Al-3Mg-MnO_2 composites.

1. Introduction

Metal Matrix Composites (MMCs) are emerging as an attractive class of materials that could synergize the properties of their constituents to create a unique combination, not available in the constituents. Aluminium alloy based composites are very appealing on account of their higher elastic modulus and strength to weight ratio, which makes them demanding in lightweight components of automobiles and aircraft applications [1]. Al-Mg alloys are non-heat treatable, and they drive their strength from solid solution strengthening, grain refinement, and strain hardening. Al-Mg alloys with low Mg content have better formability and are more suitable for large wrought products [2]. An increase in the Mg content leads to a rise of Al_3Mg_2 and Mg_5Al_8 particles in the alloy. These particles are anodic, where the initial corrosion attack takes place in the alloy [3]. The U.S. Navy spends around $2.5 billion annually in corrosion-related navy ship maintenance [4]. Al-Mg alloys become susceptible to corrosion after sensitization, and sensitization occurs if Al-Mg alloys have more than 3wt% Mg [5]. It seems worthwhile to investigate the Al-Mg-MnO_2 composite containing 3wt% Mg. The solid solubility of Mg in Al is limited to about 2wt% at 200 °C. When AA5083 alloy with 4.2 wt % of Mg is cooled rapidly from processing temperature to ambient temperature, it results in solid solution hardening. This hardening is the result of an interaction between the mobile dislocations and Mg, the solute atoms [6, 7]. The addition of manganese in Al-Mg alloys significantly increases the strength of the alloy without impacting the formability [3]. Hamid et al. [8] developed Al(Mg,Mn)-Al_2O_3(MnO_2) composites by dispersion of MnO_2 particles in Al-Mg melt and their reaction released manganese, which results in nucleation of $MnAl_6$ in the matrix. The composite shows increased strength and high ductility. Size and weight fraction of particulate have a great impact on the mechanical properties of particulate MMCs. Ghanaraja et al. [9] reported that the Al (Mg,Mn)-Al_2O_3 (MnO_2) composites reinforced with

* Corresponding author.
E-mail address: vikasnarain@yahoo.com (V. Narain).

https://doi.org/10.1016/j.heliyon.2020.e03275
Received 19 September 2019; Received in revised form 30 November 2019; Accepted 17 January 2020

nano-particles show improved strength and ductility in comparison to a composite containing coarser particles of micron size. The higher percentage of nano-particles harms strength due to the agglomeration of particles. Authors [10] in their previous work have dispersed MnO_2 in Al-8Mg alloy and found that the hardness, yield strength, tensile strength, and J_{IC} are increasing with forging while the trend of variation of these properties remains similar to their as-cast counterparts. Forging harms ductility, and it decreases with increasing MnO_2 content. The J_{IC} shows a minor dependence on the size of the reinforcement. Crack growth toughness is evaluated in terms of the non-dimensional tearing modulus [11]. Pillai et al. [12] have observed that at a given vol% of graphite, the forged composites show higher toughness than the cast composites. Balasubramaniam et al. [13] have noted that while forging the cluster of TiO_2 particles open up and resulting in voids to deteriorate the mechanical properties of Al-Zn-Mg alloy based composite.

Al-Mg alloy does not show sensitization at 3wt% Mg. Therefore, in the present study, the mechanical properties of composites synthesized by dispersing 3, 5, and 8wt% MnO_2 in Al-3Mg alloy are investigated in as-cast and forged conditions. Their mechanical properties are compared with Al-8Mg-MnO_2 composites already reported by authors in their previous work [10]. The present study also evaluates the effect of forging on mechanical properties, including elastic-plastic fracture behavior.

2. Experimental procedures

The chemical analysis of the commercially pure aluminium and magnesium ingot has been carried by using a vacuum spark emission spectrometer (Thermo Jarrell Ash, Atom Comp 181, Franklin, USA). Compositions of Al and Mg are shown in Table 1. Commercial pure aluminum containing 99.60 pct Al, 0.202 pct Fe, 0.091 pct Si, and 0.102 pct Zn, and Mg of 99.92 pct purity was used to prepare Al-3Mg alloy. The shape and size of the MnO_2 particles used for the synthesis of the Al-3Mg-MnO_2 composites are shown in Figure 1. The particle sizes in the mixture are in the range from 0.5μ to 25μ. The average particle size of the mix is 8.7 μm, as determined in a Malvern particle size analyzer–3600 E Malvern, Worcs. England. Smaller particles are round, but bigger particles are angular in shape. Stir casting, an economical and proven method, was used to synthesize the Al-3Mg-MnO_2 composite. The same process was also used to produce Al-8Mg-MnO_2 composites for relevant comparison.

In this method, Al was melted in resistance furnace, and magnesium pieces were added into molten aluminium at 800 °C. Continuous stirring at 700 rpm was maintained during the addition of preheated MnO_2 powder in the melt with the help of a motor-driven impeller. The chromel-alumel thermocouple was used for measuring melt temperature. Once the whole powder was poured, the slurry was stirred for some more minutes to obtain homogenized Al-3Mg-MnO_2 composite. The resulting slurry was cast into a water-cooled copper mold. Three different composites were synthesized with the adding of 3, 5, and 8 wt% MnO_2 particles into the Al-3Mg melt and designated as A3/3, A3/5, and A3/8 composites, respectively. These composites were tested in their as-cast and hot forged conditions. The percentage reduction after hot forging at 400 °C in A3/3, A3/5, and A3/8 composites was 22.8%, 20.0%, and 21.0%, respectively. The Brinell hardness of the composites has been measured with a 2.5 mm diameter steel ball indenter at 31.25 kg load. The tensile tests of composites were conducted on cylindrical tensile specimens of gauge length 25 mm and diameter 5 mm at a constant displacement rate of 0.2 mm/min using a universal testing machine. The length of the tensile sample used was perpendicular to the forging direction.

The *J*-integral is determined and plotted against physical crack growth, Δa_p, using at least four data points within specified limits of crack growth. Before the *J-R* test, each specimen was fatigue pre-cracked, and load-load line displacement was measured with the help of clip-gage to arrive at the *J-R* curve for the composites using a single specimen. The crack length at different load was estimated from compliance by loading-unloading at different J-values. The blunting lines were drawn at 0.2 mm offset following the equation, $J = 2\sigma_f \Delta a$, where the flow stress σ_f was equal to $(\sigma_y + \sigma_u)/2$. Where σ_y is the yield strength (N/mm^2) and σ_u is the ultimate tensile strength (N/mm^2). The program determines the exact point of intersection of the *J-R* curve with the blunting line. All the tests conducted in this study satisfy plain strain criterion.

3. Results and discussion

The optical microstructure of a typical as-cast A3/5 composite is shown in Figure 2 (a). The dark particles in the microstructure are reasonably well distributed in the matrix. Figure 2 (b) shows an etched micrograph, which reveals grain boundaries, precipitates within the grains, and along the grain boundary. The voids and pits are also clearly visible in Figure 2 (b). The reason behind this observation is the removal of precipitates from these sites during polishing or etching activity.

Clusters of MnO_2 particles are increasing as the MnO_2 content is increasing in the composite. These clusters are nothing but a combination of many particles at one place, or individual particles spread closely at a particular location. As the amount of MnO_2 increases from 3 to 8 wt%, there is an increase in clustering. A typical optical microstructure of A3/8 composite representing such clustering is shown in Figure 3 (a). The particle-matrix interface cohesiveness is not very clear at low magnification in Figure 3 (a).

The dark portions at higher magnification in Figure 3(b) suggest the existence of voids at the interface as well as around the segregated particles. In this way, it is evident that wherever there is segregation, the cohesiveness of the interface will be very poor. Forging plays a crucial role in reducing voids or pores in the composite. Nevertheless, there is no guarantee that it will eliminate or cure all the pores. A typical micrograph, as shown in Figure 4, reveals that the forging has fractured the particles and could not heal the voids in the matrix. The broken particles act as the site of fracture nucleation and facilitate early fracture. Consequently, it decreases the strength of the composite.

Both sets of composites, Al-8Mg-MnO_2 and Al-3Mg-MnO_2, show similar precipitates within grains, and along the grain boundary. Forging helps in reducing the voids in both the set of composites and fractured particles during the forging operation. The EDX analysis conducted on the A3/5 composite is shown in Figure 5. Figure 5(a) shows small alumina particles embedded in the matrix. It may be in-situ alumina because the *in-situ*-grown composites show clean interfaces, strong interfacial bonding, and a narrow particle size distribution [14]. Figure 5 (b) shows the MnO_2 particle, which has partially reacted Mg in the form of MgO. Figure 5 (c) shows MnO_2 particle and possible intermetallic compound of Al and Mg. Figure 5(d) shows the presence of MgO particle, and Figure 5 (e) reveals the unreacted MnO_2 particle.

The X-ray diffraction pattern indexing of the extracted particles obtained after leaching the composite Al-3Mg-MnO_2 has been done manually with the help of JCPDC data cards. The interplaner distance d,

Table 1. Chemical composition of the commercial aluminium and magnesium.

Material	Chemical composition								
	Si	Fe	Zn	Cr	Ti	Mn	Cu	Mg	Al
Al-Ingot	0.091	0.202	0.102	0.002	0.006	0.020	0.001	0.001	Bal.
Mg-Ingot	0.007	0.021	0.003	0.000	0.002	0.001	0.018	Bal.	0.025

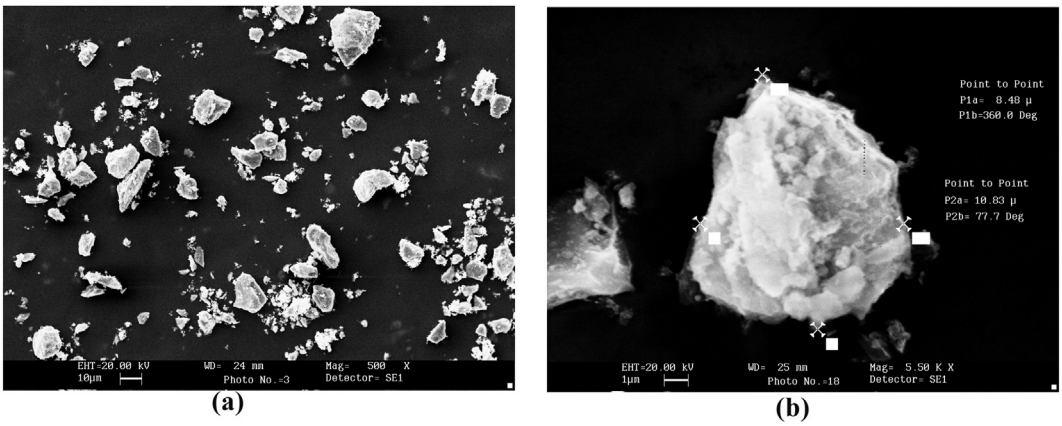

Figure 1. (a) Micrograph of MnO_2 powder used for the synthesis of Al-3Mg-MnO_2 composite. (b) MnO_2 particles at higher magnification.

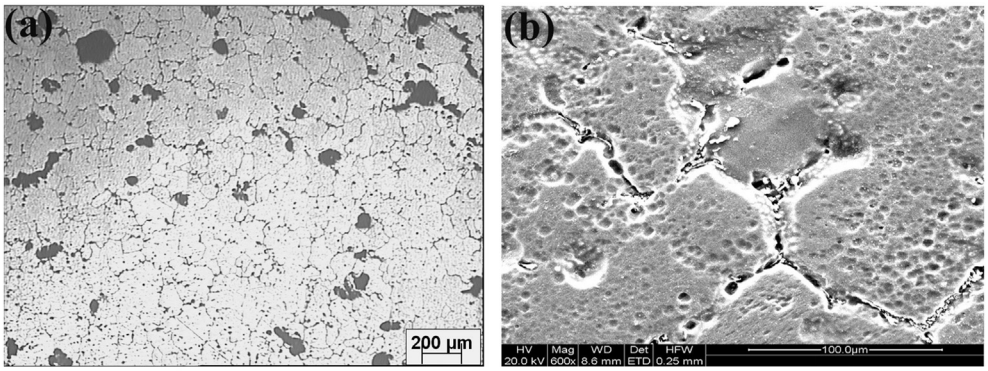

Figure 2. Microstructure of as-cast Al 3/5 composite etched with HF at (a) relatively lower magnification and (b) SEM micrograph at higher magnification.

corresponding 2θ, and identified phases are listed in Table 2. The table suggests the presence of oxides of Al, Mg, and Mn. These phases are similar to phases, as reported in Al-8Mg-MnO_2 composite in their X-ray diffraction analysis.

The Brinell hardness of cast and forged Al-3Mg-MnO_2 composites are shown in Table 3. It also shows a number of oxides obtained from these composites after acid leaching. These oxides are a mixture of MgO, $MgAl_2O_4$, Al_2O_3, and MnO_2. Dark shades in the optical micrograph are the representation of oxide particles. The dark particles of oxides formed in A3/3 and A3/5 composites are shown in Figure 6.

The Al-3Mg-MnO_2 and Al-8Mg-MnO_2 composites both have similar oxide particles and intermetallics, but they differ in the extent of greyish precipitates in the composites. The grayish precipitates are possible of Al_3Mg_2 in the optical micrograph. The greyish precipitates in Al-3Mg-MnO_2 composites are relatively less than that of Al-8Mg-MnO_2 composites.

The fractograph of specimens used for the tensile test is shown in Figure 7. In all the samples, necking is very prominent, clear, and decreasing as the percentage of MnO_2 is increasing from 3 to 8 wt%, as shown in Figure 7 (a,c,e). The composite A3/3 in Figure 7 (b) shows several dimples, a sign of ductile fracture and high ductility, throughout the sample. The composite A3/5 in Figure 7 (d) shows less number of dimples. These dimples are flat at the peak, as it loses its plasticity after some elongation. The fractured sample of composite A3/8 in Figure 7 (f) shows a minimal number of dimples. There is a variation of the size of dimples from small to big ones. In all the three samples of Al-3Mg-MnO_2 composites, A3/3 shows the highest ductility. The tensile specimens of Al-8Mg-MnO_2 composites were less ductile, and therefore minute

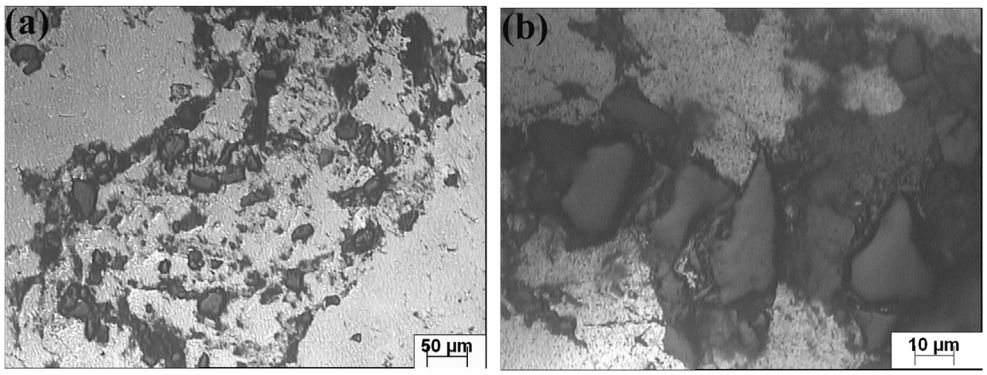

Figure 3. MnO_2 particle distribution (a) Segregated particles at low magnification, (b) Particles at higher magnification.

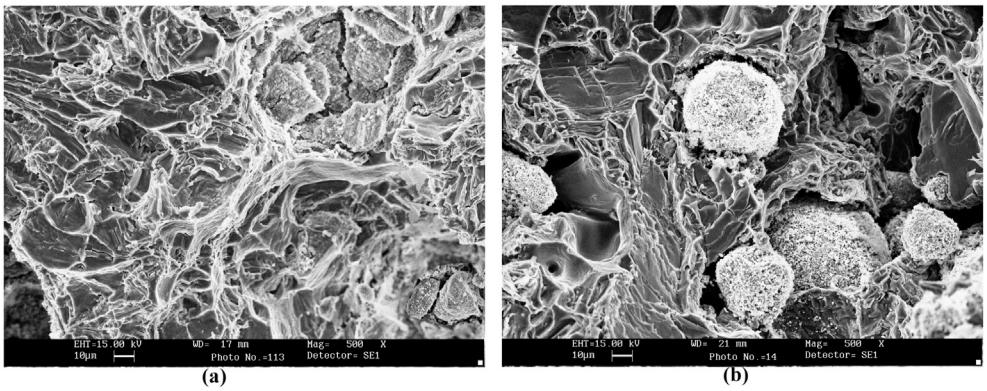

Figure 4. SEM micrograph of forged composite (a) Fractured particle (b) Unhealed pores around particles.

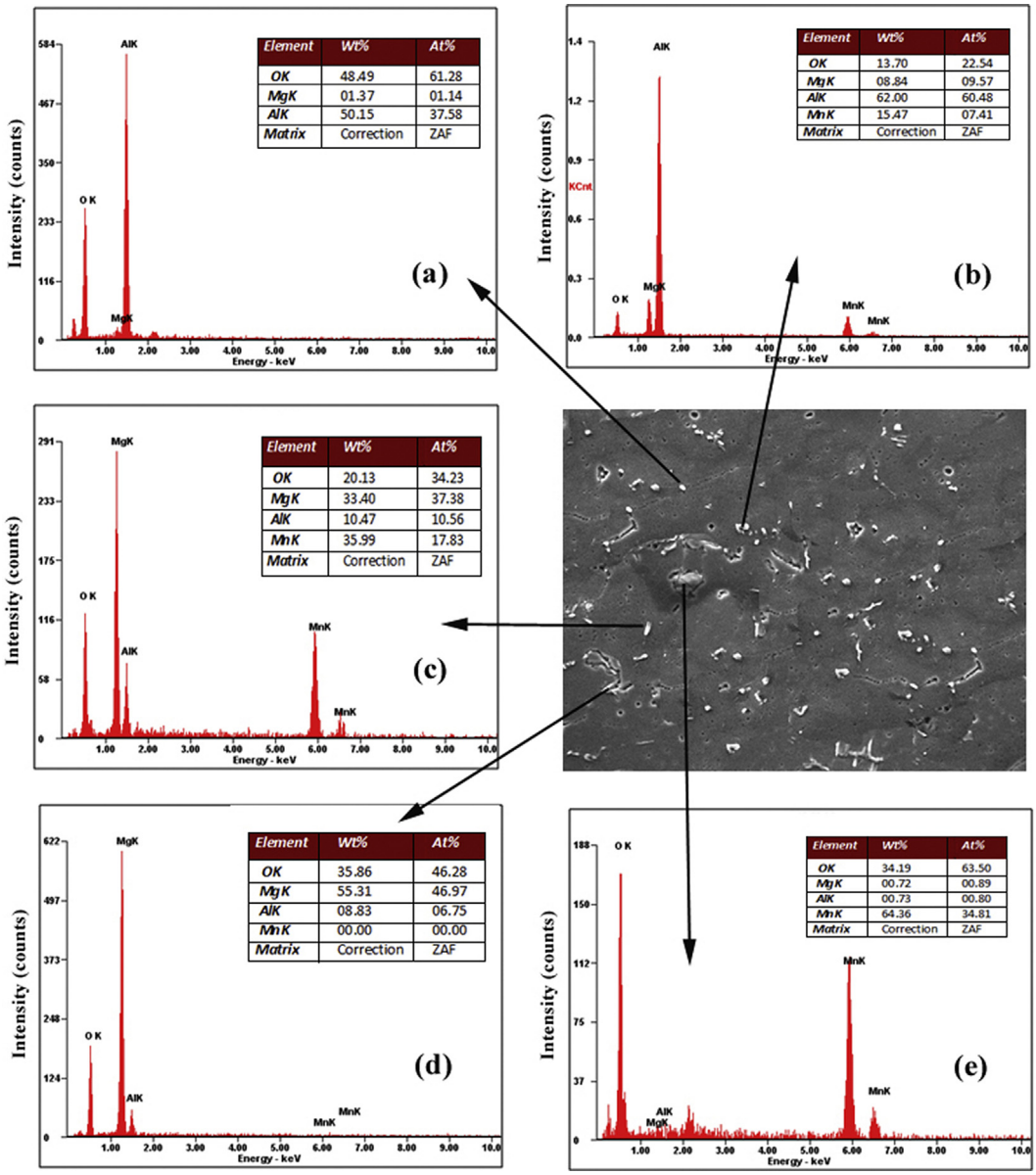

Figure 5. EDX analysis of Al-3Mg-MnO_2 composite. (a) Al_2O_3 particles (b) MnO_2 and partially reacted MgO (c) MnO_2 and intermetallic of Al and Mg (d) MgO particle (e) unreacted MnO_2 particle.

Table 2. X-ray diffraction analysis for particles extracted from in-situ composites of Al(Mg)-(MnO_2) Composite.

d (A^0)	2θ (degree)	Phases, intensities [ ]and its (h k l) values
4.79	18.47	$MgAl_2O_4$ [10] (002)
3.11	28.65	βMnO_2 [100] (110), $MgAl_2O_4$[80] (202),
2.81	31.80	θAl_2O_3 [80] (401+), γAl_2O_3 [45] (220)
2.40	37.36	θAl_2O_3 [60] (111), β MnO_2 [55] (101), γAl_2O_3 [65] (311), $MgAl_2O_4$ [20] (302), MgO [10] (111), αAl_2O_3[40](110)
2.10	42.68	βMnO_2 [16](111), $MgAl_2O_4$ [100] (303), MgO [100] (200), αAl_2O_3[100](113), θAl_2O_3[45](311-,112-)
1.98	45.68	γAl_2O_3 [80] (400), βMnO_2 [5] (210), θAl_2O_3 [30] (600) αAl_2O_3 [2](202)
1.53	60.37	γAl_2O_3 [10] (511), θAl_2O_3 [25] (313), βMnO_2 [14] (220), αAl_2O_3 [4](211)
1.42	65.21	γAl_2O_3 [100] (440), $MgAl_2O_4$ [30] (413), MgO [52] (220), αAl_2O_3[30](124)
1.39	66.86	θAl_2O_3 [100] (712-,512+), βMnO_2 [20] (301), $MgAl_2O_4$ [25] (504), αAl_2O_3[50](030)

Table 3. The Brinell hardness of as cast and forged composites.

Composite Designation	Oxide content in wt%	Brinell Hardness (BHN)	
		As Cast Composite	Forged Composite
A3/3	3.3	35.14	58.21
A3/5	4.5	60.2	63.3
A3/8	6.1	65.3	61.8

necking was seen in those samples in comparison to specimens of Al-3Mg-MnO_2 composites.

The hardness of Al-3Mg-MnO_2 and Al-8Mg-MnO_2 composites are shown in Figure 8. The hardness of Al-3Mg-MnO_2 based composites increases as the oxide content increases.

The hardness of particulate composites depends on many factors such as hardness of reinforcement, the extent of grain refinement, impeding of dislocation, and how effectively load is being transferred from matrix to reinforcement [15]. The Al-3Mg-MnO_2 composite, which has 3wt% Mg, forms a substitutional solid solution with Al as its atomic radius is 16% larger than that of Al atom. It creates stress in the lattice and results in solid solution strengthening, which increases hardness as well as strength. MnO_2 reacts with Al and produces in-situ Al_2O_3 and releases Mn in the matrix. As the percentage of MnO_2 increases, there is an increase in the amount of Al_2O_3 and Mn released in the matrix. The presence of intermetallic phases Al_3Mg_2, $AlMn_6$, and intermetallic formed due to impurities like Fe, and Si also helps in increasing hardness. Though hardness increases with increasing oxide content, but it increased to 71.42% at 5wt% MnO_2 in comparison to the hardness at 3wt% MnO_2. As the MnO_2 content increased to 8wt%, the increase in hardness was just 8.33% in comparison to hardness at 5wt%. The agglomeration of particles is more prominent at higher oxide content, and the concentration of pores is around these agglomerations (Figure 3). A high hardness was expected at 8wt% MnO_2 as it has more oxides than 5wt% MnO_2 composite, but high porosity has negated his advantage. Due to this reason, 5wt% MnO_2 composite is showing higher hardness. After forging, the hardness increases significantly in the composite containing 3wt% oxides, which may be due to the work hardening as well as the healing of porosity. However, in composite containing 5wt% oxides, there is only a marginal increase in hardness compared to corresponding as-cast composite. The marginal increase is possibly due to the balancing of work hardening by the healing of pores. After forging, porosity engulfed particles do not get enough support from the matrix to contribute to the hardness, and broken particles also harm hardness, as evident from Figure 8. In Al-8Mg-MnO_2 composites, there is a linear increase in hardness with an increase in MnO_2. Forging has correspondingly increased the hardness, as observed in as-cast composites. This linearity of hardness is not visible in Al-3Mg-MnO_2 composites.

The variations of yield strength, tensile strength, and percentage elongation of Al-3Mg-MnO_2 and Al-8Mg-MnO_2 with increasing particle content in both the forged and cast conditions are shown in Figures 9, 10, and 11, respectively. In Figure 9, the yield strength of Al-3Mg-MnO_2 is increasing with increasing particle content in the composites.

Enhanced particle content increases nuclei sites for solidification and results in smaller grain sizes, as evident in Figure 6. Increased MnO_2 particles also provide more manganese alloying elements in the matrix, which increase solid solution strengthening. The presence of oxide particles, Al_3Mg_2, and $AlMn_6$ has a pinning effect in the movement of dislocation. The dislocations also experience hindrance while moving from one grain to the next because of abrupt change in the orientation of planes, and it increases the yield strength. Smaller the grain size, more the hindrance in dislocation movement and yield strength increases as per Hall-Petch relation: $\sigma_y = \sigma_i + k/\sqrt{d}$ where σ_y yield strength, d is is grain diameter, σ_i and k are constants. As the oxide particle increases from 3wt% to 5wt%, a rise of 19.66% in yield strength is observed, but a further increase of oxide particle to 8wt% marks a tremendous growth of 128.38% in yield strength. At 5wt% oxide content, an increase in yield is

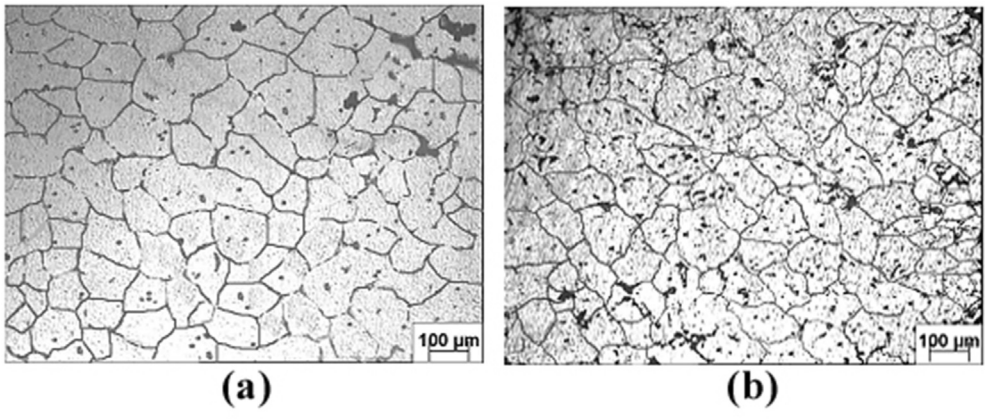

Figure 6. Optical micrograph of (a) A3/3 composite (b) A3/5 composite.

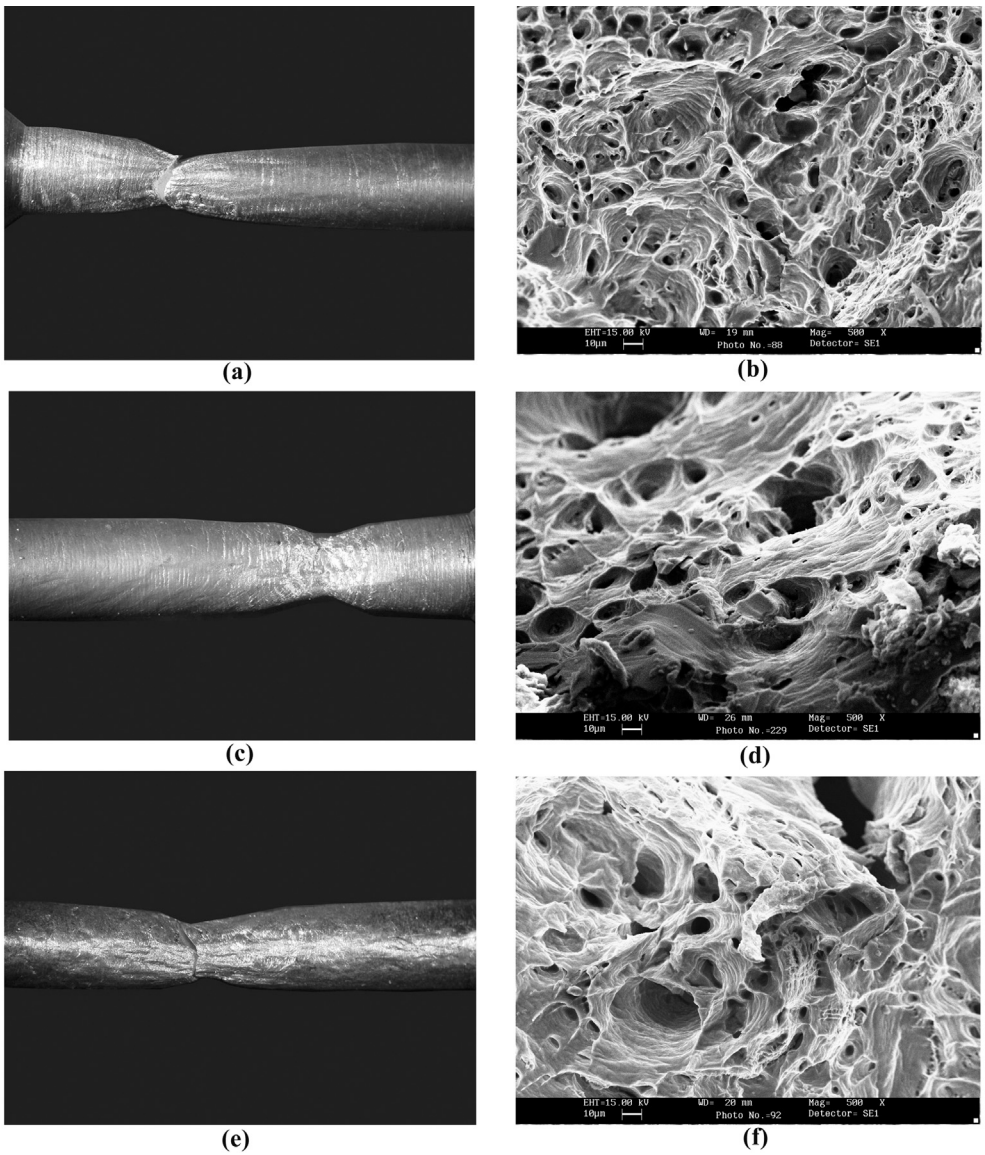

Figure 7. Fractograph of Al-3Mg-MnO_2 composite. (a) The tensile sample of A3/3 (b) fractograph of sample A3/3 (c) The tensile sample of A3/5 (d) fractograph of sample A3/5 (e) The tensile sample of A3/8 (f) fractograph of sample A3/8.

because of the presence of more oxide particles, which have reduced the grain size and inhibited the movement of dislocation. At 8wt% MnO_2 content, a steep increase is probably because of further reduction of grain size. At this level, it does not follow linear increase but increases significantly, as also suggested by Nagai et al. for recrystallized grains [16]. After forging, the yield strength increases with increasing particle content almost linearly. Forging has improved the yield strength by 36.1% and 47% in comparison to their cast counterpart of A3/3 and A3/5 composites. But forged A3/8 composite shows a reduction of 11.09% in its yield strength in comparison to their cast counterpart. The decrease at 8wt% MnO_2 is because of unhealed pores which do not provide strain hardening. In Al-8Mg-MnO_2 composites, there is a linear increase in yield strength with an increase in MnO_2 content. Forging has further increased the yield strength, and followed the similar trend, as observed in the as-cast composite. The Al-3Mg-MnO_2 composites show a linear increase only in forged condition but not in cast conditions. The yield strength values of Al-8Mg-MnO_2 composites are very high in comparison to Al-3Mg-MnO_2 composites.

The presence of fine reinforcement causes Orowan strengthening and refines gain size. It has strengthening effect in particulate metal matrix composite. The reinforcement particles always have a mismatch of elastic and coefficient of thermal expansion with the matrix, and it enhances the strength of the composite [15]. Variation of tensile strength in Al-3Mg-MnO_2 composites with MnO_2 content is shown in Figure 10. The tensile strength of cast Al-3Mg-MnO_2 composites increases by 8.77% when oxide content increases from 3 to 5 wt%, but further increase in particle content to 8 wt% has increased the tensile strength by 2.92%.

This adverse effect may be due to enhanced porosity (Table 4), which acts as fracture initiating sites and lowers the tensile strength. The tensile strength is higher in forged composites and increases with increasing particle content from 3 to 5 wt%. This increase is 16.97% and 13.49% in comparison to their cast counterparts. However, as the oxide particles increase to 8 wt%, there is a fall of 4.97% in contrast to cast counterpart. Healing of pores is more at the lower MnO_2 content, and this healing is more partial or incomplete at higher MnO_2 content. After forging, unweld pores act as a point of stress concentration to initiate fracture at an early stage and reduces the tensile strength. Effective stress transfer from matrix to the reinforcements governs tensile strength and this transfer take place once the matrix strain hardening reaches to its saturation. At this stage, all the load is borne by the reinforcements, and as the few particle fractures, the total load shifts to neighbor particles, which leads to cascading effect of particle fracture and, ultimately,

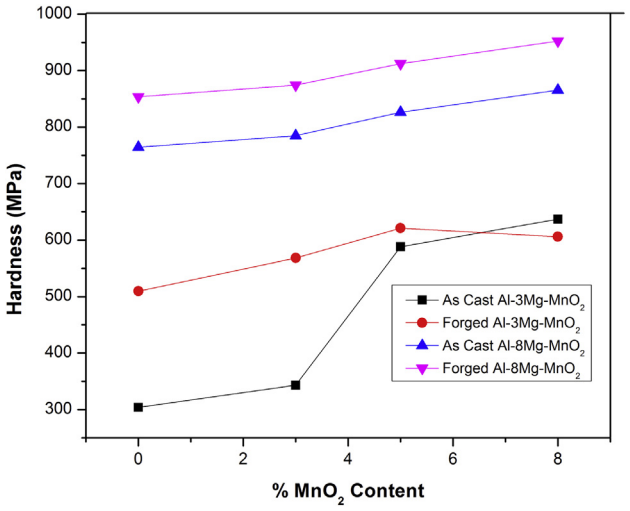

Figure 8. The Hardness of as-cast and forged Al-3Mg-MnO_2 and Al-8Mg-MnO_2 composites with MnO_2 content.

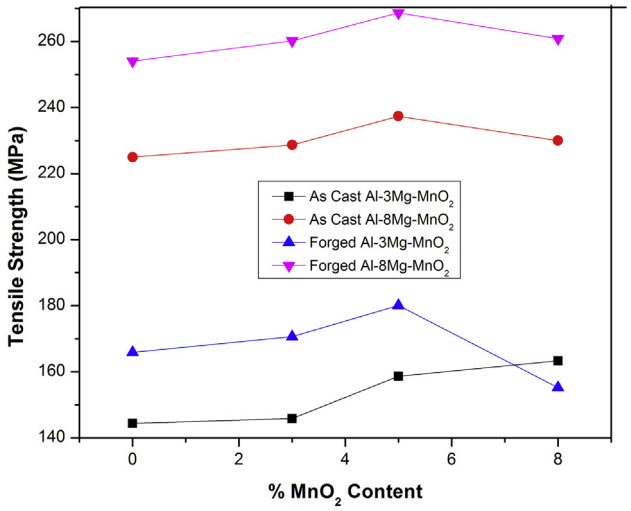

Figure 10. Variation of tensile strength in as-cast and forged Al-3Mg-MnO_2 and Al-8Mg-MnO_2 composites with MnO_2 content.

tensile specimen fractures [17]. At 8wt% of MnO_2, forged composite had fractured particles and unhealed pores at the particle-matrix interface. This gap does not allow passing the load effectively on reinforcement particles, and interfacial pores themselves start acting as fracture nucleation sites before being transferring the load to the reinforcement particles. Due to this reason, it has reduced the tensile strength. When the tensile strength of Al-3Mg-MnO_2 is compared with Al-8Mg-MnO_2 composites, it is found that the tensile strength of Al-3Mg-MnO_2 composites increases with increasing particle content in their cast and forged conditions, but at 8wt% particles, there is a decrease in tensile strength after forging in comparison to cast counterpart. Whereas in Al-8Mg-MnO_2 composites, the tensile value increases with particle content from 3 to 5 wt%, but there is a sharp reduction at 8wt%. Forging has improved the tensile values, but the trend remains the same as of cast composite.

The matrix strength, strain hardening capacity, reinforcement volume fraction, shape, size, and spatial distribution are important parameters that affect the ductility of the composite [17]. In Figure 11, the % elongation of Al-3Mg-MnO_2 composites is decreasing with increasing oxide content because the size of the grain is decreasing with increasing oxide content.

Smaller grains have more boundaries than larger grains; therefore, they create more hurdles in the path of dislocation movement than the

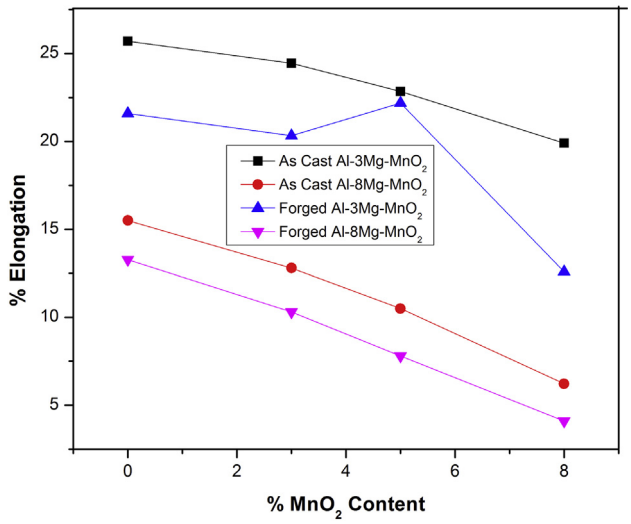

Figure 11. Variation of percentage elongation in as-cast and forged Al-3Mg-MnO_2 and Al-8Mg-MnO_2 composites with MnO_2 content.

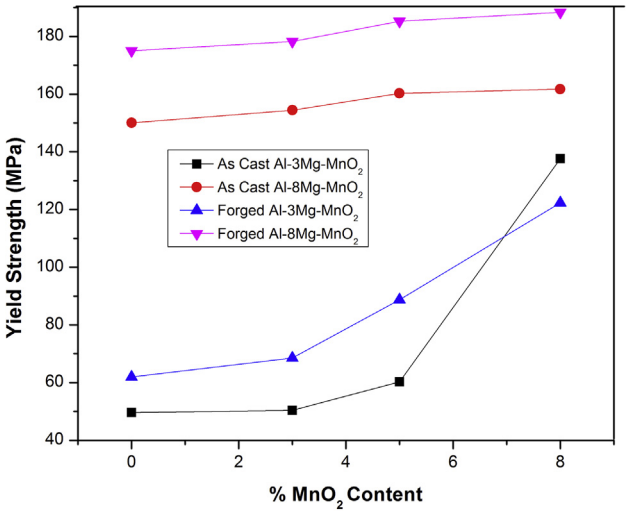

Figure 9. The yield strength of as-cast and forged Al-3Mg-MnO_2 and Al-8Mg-MnO_2 composites with MnO_2 content.

large grains. This obstruction leads to a decrease in ductility. Forging increases work hardening, reduces pores, and restricts the movement of dislocation. The forged composite shows much lower ductility than the cast composites. Forging has reduced the percentage elongation of A3/3 composite by 16.89%. However, forged A3/5 composite shows meagre reduction of 2.93%. It gives the sense that A3/5 composite has more percentage elongation in comparison to forged A3/3 composite. Forged A3/8 composite shows a reduction of percentage elongation by 36.78% in comparison to its cast counterpart. The work hardening in forged A3/3 is more than forged A3/5 composite because the porosity content is more at higher particle content. The work hardening in forged A3/8 composite

Table 4. Porosity in cast and forged composites.

Sample	Percentage Reduction in Forging	Porosity	
		Cast	Forged
AM3O3	22.8	3.60	2.89
AM3O5	20.0	5.70	4.98
AM3O8	21.0	7.66	7.1

is least in comparison to A3/3 and A3/5 composites. Nevertheless, it is not showing the highest % elongation because the sample was broken due to porosity before it could yield more ductility. Unhealed pores had a detrimental effect at this stage and led to a quick fracture of the sample. Due to this reason, after forging, the % elongation reduction in A3/5 composite is less than the A3/8 composite. The percentage elongation of Al-8Mg-MnO_2 composites also decreases with increasing MnO_2 content, and forging reduces it further. However, the trend of decrease remains linear and similar to its cast counterparts. The lowest value of percentage elongation is 4.1% in forged Al-8Mg-MnO_2 composite, whereas it is 12.6% in Al-3Mg-MnO_2 composite.

The J-R curves of as-cast and forged Al-3Mg-MnO_2 composites containing 3, 5, and 8 wt% MnO_2 particles are shown in Figure 12 (a), (b) and (c), respectively.

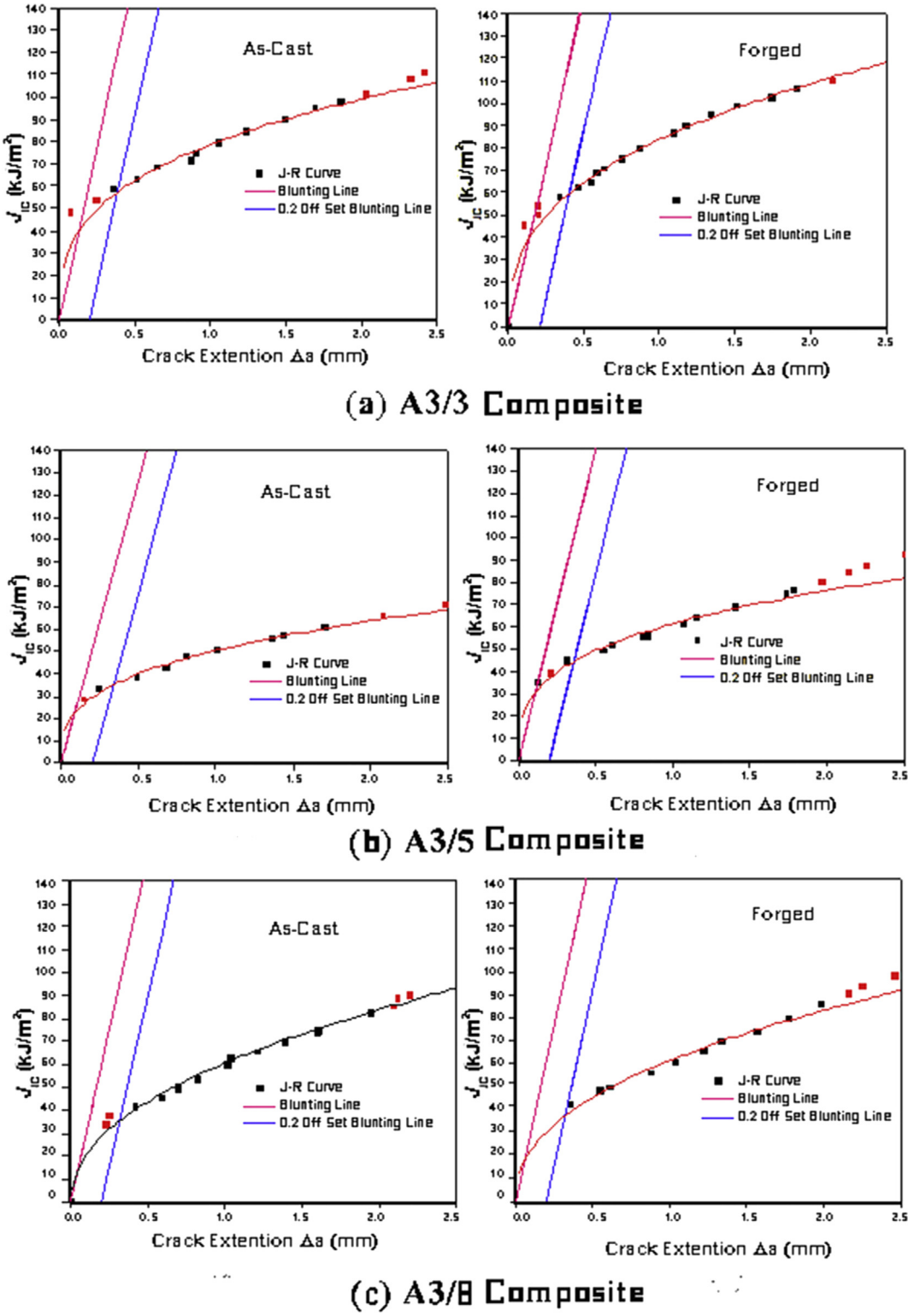

Figure 12. *J-R* curves of as-cast and forged Al-3Mg-MnO_2 composites with different particle contents: (a) A3/3 composite, (b) A3/5 composite and (c) A3/8 composite.

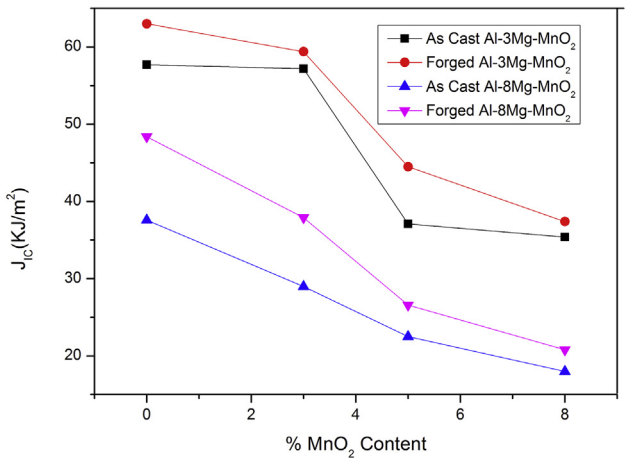

Figure 13. Variation of fracture toughness, J_{IC} of as-cast, and forged Al-3Mg-MnO_2 and Al-8Mg-MnO_2 composites with MnO_2 content.

The initiation of fracture does not take place simultaneously across the entire crack front, an offset of 0.2 mm is taken to draw the blunting line, and its intersection with the *J-R* curve indicates the initiation fracture toughness, J_{IC}. Variation of Initiation fracture toughness, J_{IC} of the cast, and forged Al-3Mg-MnO_2 and Al-8Mg-MnO_2 composites with MnO_2 particle content are shown in Figure 13.

The J_{IC} values decrease as the percentage of MnO_2 particles increases in Al-3Mg-MnO_2 composites. Forging has increased J_{IC} values in comparison to their cast counterparts, but the trend of decrease with increasing MnO_2 content remains the same as of cast composite. A similar result is seen in Al-8Mg-MnO_2 composite, where forging has increased the J_{IC} values, but the extent of the increase, decreases as the percentage of particles increases and overall trend remains similar to as-cast composite. In both the cases, forging has improved the J_{IC} value, the reason behind this observation may be work hardening and healing of the pores after the forging. The ratio of tearing modulus to elastic modulus may be considered as crack growth toughness of the material. The T/E ratio of Al-3Mg-MnO_2 and Al-8Mg-MnO_2 composites are shown in Figure 14.

Crack growth toughness is decreasing as the MnO_2 particle is increasing in Al-3Mg-MnO_2 composite. Forging has further reduced the crack growth toughness values in comparison to their cast counterparts. This decrease of the T/E ratio with increasing MnO_2 content is similar to as-cast composite except at 8wt%. The forged Al-8Mg-MnO_2 composite shows an enhanced T/E ratio in the initial stage, but at higher MnO_2 percentage, there is a decrease in the T/E ratio in comparison to their as-cast counterpart. Variation of crack growth toughness between cast and forged Al-8Mg-MnO_2 is minimal in comparison to range between cast and forged Al-3Mg-MnO_2 composite.

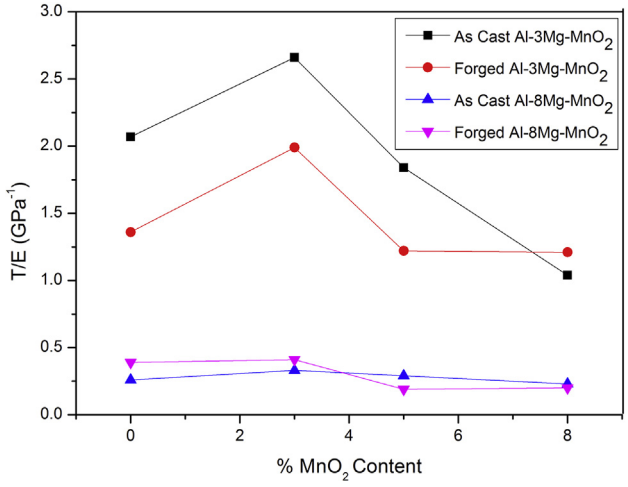

Figure 14. The T/E ratio for as cast and forged Al-3Mg-MnO_2 and Al-8Mg-MnO_2 composites with MnO_2 content.

4. Conclusion

A comparison of mechanical properties of Al-3Mg-MnO_2 and Al-8Mg-MnO_2 composites which were made by the addition of 3, 5, and 8 wt% MnO_2 in Al-3Mg and Al-5Mg alloy have led us to the following conclusions:

1. The microstructure of both sets of composites shows intermetallic precipitates containing Al, Mg, and Mn at dendrite boundaries and within grains. Hardness increases with increasing MnO_2 content in the composites. Forging has improved it further, but this improvement is more prominent in Al-3Mg-MnO_2. At higher content, healing of pores is not that effective, and this results in a moderate increase in hardness.
2. The yield strength increases linearly with increasing MnO_2 in forged and cast Al-8Mg-MnO_2 composites. The Al-3Mg-MnO_2 composites show a linear increase only in a forged condition, not in cast conditions. The yield strength values are very high in Al-8Mg-MnO_2 composites in comparison to Al-3Mg-MnO_2 composites.
3. The tensile strength of Al-3Mg-MnO_2 composites increases with increasing particle content, but at 8wt.% MnO_2 content, there is a decrease in tensile strength in forged condition. Whereas in Al-8Mg-MnO_2 composites, tensile strength increases with particle content from 3 to 5 wt% and reduces at 8wt % in both forged and cast conditions.
4. Both the set of composites show a linear decrease in % elongation as the MnO_2 content increases in the as-cast condition. Forging further reduces the % elongation linearly in Al-8Mg-MnO_2 composites. In the case of Al-3Mg-MnO_2 composite, forging has decreased % elongation at 3, and 8wt% MnO_2 content but an improvement is observed at 5wt %. The lowest value of percentage elongation is 4.1% in the case of forged Al-8Mg-MnO_2 composites, whereas it is 12.6% in Al-3Mg-MnO_2 composite.
5. The J_{IC} value decreases as the percentage of MnO_2 particles increases in Al-3Mg-MnO_2 and Al-8Mg-MnO_2 composites. Forging has increased J_{IC} values in both the set of composites in comparison to their cast counterparts. This increase may be due to work hardening and healing of the pores after the forging.
6. Crack growth toughness decreases as the MnO_2 particle increases in Al-3Mg-MnO_2 and Al-8Mg-MnO_2 composites. Forging of Al-3Mg-MnO_2 decreases the T/E ratio in comparison to their cast counterpart except at 8wt%. However, forging of Al-8Mg-MnO_2 has improved T/E at lower MnO_2 content and decreased at 5 and 8wt% MnO_2. Variation of crack growth toughness between cast and forged Al-8Mg-MnO_2 is minimal in comparison to range between cast and forged Al-3Mg-MnO_2 composites.

Declarations

Author contribution statement

Vikas Narain: Conceived and designed the experiments; Performed the experiments; Analyzed and interpreted the data; Wrote the paper.

Subrata Ray: Conceived and designed the experiments; Contributed reagents, materials, analysis tools or data.

Funding statement

This research did not receive any specific grant from funding agencies in the public, commercial, or not-for-profit sectors.

Competing interest statement

The authors declare no conflict of interest.

Additional information

No additional information is available for this paper.

References

[1] S. Ray, Casting of metal matrix composites, in: G.M. Newaz, H. Neber-Aeschbacher, F.H. Wohlbier (Eds.), Metal Matrix Composites, Part 1 : Applications and Processing, Trans Tech Publications, 1995, pp. 417–446.

[2] J. Zhang, J.J. Zhao, R.L. Zuo, Microstructure and mechanical properties of micro-alloying modified Al-Mg alloys, in: Proceedings of the 2015 International Conference on Power Electronics and Energy Engineering, 20, 2015, pp. 153–156.

[3] N.E. Idenyi1, P.A. Nwofe1, P.E. Agbo1, B.J. Ifeanyichukwu1, C.O. Ozibo1, Effects of manganese addition on the corrosion behaviour of aluminium alloys in different media, Asian J. Appl. Sci. 3 (2015) 514.

[4] E.F. Herzberg, E.D. Ambrogio, C.L. Barker, E.F. Harleston, W.M. Haver, R.J. Marafioti, G.L. Stimatze, T. Andrew, J.C. Tran. The Annual Cost of Corrosion for Army Ground Vehicles and Navy Ships, Report SKT50T1, LMI Government, 2006.

[5] A.J. Davenport, Y. Yuan, R. Ambat, B.J. Connolly, M. Strangwood, A. Afseth, G. Scamans, Intragranular corrosion and stress corrosion cracking of sensitized AA5182, Mater. Sci. Forum 519–521 (July) (2006) 641–646.

[6] I.N.A. Oguocha, O.J. Adigun, S. Yannacopoulos, Effect of sensitization heat treatment on properties of Al–Mg alloy, J. Mater. Sci. 43 (Online Issue) (2008) 4208–4214.

[7] Øyvind Ryen, Hans Ivar Laukli, Bjørn Holmedal, Erik Nes, Large strain work hardening of aluminum alloys and the effect of Mg in solid solution, Metall. Mater. Trans. 37 (A) (2006) 2007–2013.

[8] A. Hamid Abdulhaqq, P.K. Ghosh, S.C. Jain, S. Ray, Processing Microstructure and mechanical properties of cast in-situ Al(Mg, Mn)-Al_2O_3(MnO_2) Composite, Metall. Mater. Trans. A 36A (2005) 2211–2223.

[9] S. Ghanaraja, S.K. Nath, S. Ray, Processing and mechanical properties of cast Al (Mg, Mn)-Al_2O_3 (MnO_2) composites containing nanoparticles and larger particles, Metall. Mater. Trans. A 45A (2014) 3467.

[10] V. Narain, S. Ray, "Variation in Mechanical Properties with MnO_2content in Cast and Forged In-Situ Al-8Mg-MnO_2composites" Journal of Materials Research and Technology, 2019. Article in press.

[11] M. Manoharan, J.J. Lewandowski, Crack initiation and growth toughness of an aluminum metal matrix composite", Acta Metall. Mater. 38 (3) (1990) 489–496.

[12] U.T.S. Pillai, R.K. Pandey, P.K. Rohatgi, Effect of volume fraction and size of graphite particulates on fracture behaviour of AL-graphite composites, Eng. Fract. Mech. 28 (4) (1987) 461–477.

[13] P.K. Balasubramanian, Rao P. Srinivasa, K.G. Sivadasan, K.G. Sathyanarayana, B.C. Pai, P.K. Rohatgi, Forging characteristics of Al-Zn-Mg alloy containing 5 wt% TiO_2 dispersion, J. Mater. Sci. Lett. 8 (1989) 799–801.

[14] R. Asthana, Review Reinforced cast metals Part I Solidification microstructure, J. Mater. Sci. 33 (1998) 1679–1698.

[15] S. Sankaranarayanan, S. Jayalakshmi, Manoj Gupta, Enhancing the ductility of Mg-(5.6Ti+3Al) composite using nano-B_4C addition and heat treatment, SOJ Materials Science & Engineering, 2013.

[16] Manabu Nakai, Goroh Itoh, The effect of microstructure on mechanical properties of forged 6061 aluminum alloy, Mater. Trans. 55 (1) (2014) 114–119.

[17] J. Llorca, C. Gonzalez, Microstructural factors controlling the strength and ductility of particle reinforced metal-matrix composites, J. Mcch. Phys. Solids 46 (I) (1998) I–28.